Supporting Information for

Photoswitching Dynamics of a Guanidine Anion Receptor

Ying-Zhong Ma*[1], Jeffrey D. Einkauf,[1] Xinyou Ma,[1] Duy-Khoi Dang,[2] Paul M. Zimmerman,[2] Radu Custelcean,[1] Benjamin Doughty,[1] Vyacheslav S. Bryantsev*[1]

[1]Chemical Sciences Division, Oak Ridge National Laboratory, P.O. Box 2008, Oak Ridge, TN 37831

[2]Department of Chemistry, University of Michigan, Ann Arbor, MI 48109, USA

*Corresponding authors

This PDF file includes:

Supplementary Text

Supplementary Figure S1 and S8

Supplementary Reference

ASSOCIATED CONTENT

Supplementary Information:

Description of the nanosecond transient absorption method and results; definition of rection coordinate in *E,E* → *E,Z* isomerization; the transition states in *E,E* → *E,Z* isomerization; supplementary figures showing (S1) relative free energies of triflate (OTF) complexes with 2PyDIG in the *E,E* form and free ligands in the *Z,Z* form in DMSO solvent; (S2) the CASSCF active orbital rendered at 0.0 isosurface, electron occupations, and orbital energies of the optimized *E,E* isomer at SA2-CAS(13,12)SCF/6-31G** level of theory; (S3) steady-state fluorescence excitation spectra before and after light illumination to induce the *E,E* ® *Z,Z* photoisomerization using a xenon lamp for 90 minutes; (S4) reconstructed time-resolved fluorescence spectra using the TCSPC data measured upon excitation at 356 nm and 336 nm, respectively; (S5) contour plot of nanosecond transient absorption signal versus probe wavelength and delay time obtained upon optical excitation with a nanosecond laser at 355 nm; (S6) nanosecond transient absorption kinetics acquired for 2PyDIG/DMSO solution and pure DMSO solvent at 360 nm; (S7) optimized structures of the most stable conformers of the *E,E* and *Z,Z* forms and the selected geometric parameters in the ground (S_o) and the first excited (S_1) states; and (S8) 2-dimensional potential energy surface (PES) of the *E,E*-2PyDIG isomer in S_1 electronic excited state as a function of C–N distance and N-N-C-C dihedral angle, along with the potential energies at ϑ_{NNCC} = 180 degrees as a function of C=N distance.

1. Supplementary Text

Nanosecond Transient Absorption

To determine an efficient intersystem crossing (ISC) can take place, we performed nanosecond transient absorption measurements upon 355 nm optical excitation, which would enable us to probe triple state via either ground state recovery or/and triplet-triplet excited-state absorption processes. A commercial laser flash photolysis system (LFP-112, Luzchem) in transmission mode was used, which employs the third (355 nm) harmonic output of a Q-switched Nd:YAG laser producing ~5 ns pulses with 4 mJ pulse energy (Minilite I, Continuum) as the optical pump pulses. The probe beam was provided by a 175 W ceramic xenon lamp and delivered through fiber-optic cables. The pump laser was synchronized with the LFP-112 system and a repetition rate of 0.5 Hz was chosen to allow the fresh, unexcited portion of sample diffuse into the excited volume during the laser pulses. As photoisomerization takes place quickly under this laser excitation condition, care was exercised to ensure that majority of the molecules remains as *E,E* isomer

during the data acquisition. For this reason, each freshly prepared sample solution was used in a measurement for ~ 2 min only.

Definition of Rection Coordinate in E,E → E,Z Isomerization

To illustrate the four minimum free energy paths in a combined scheme of potential energy curve (see Figure 10), we define the reaction coordinate *R*c as a function of r_{CN}, θ_{NNCC}, and r_{NH}:

$$R_C(r_{CN},\theta_{NNCC},r_{NH}) = \begin{cases} \dfrac{r_{CN}-r_1}{r_2-r_1}\cdot\delta(\theta_{NNCC}-\pi) \\ (1-\theta_{NNCC}/\pi)+1 \\ \dfrac{r_2-r_{CN}}{r_2-r_1}\cdot\delta(\theta_{NNCC}-0)+2 \\ \left(\dfrac{r_{NH}-r_4}{r_3-r_4}\right)\cdot\delta(\theta_{NNCC}-0)+3 \end{cases} \quad (S1.1)$$

where δ is a delta function, r_1 = 1.30 Å, r_2 = 1.42 Å, r_3 = 1.01 Å, and r_4 = 2.17 Å.

The Transition States in E,E → E,Z Isomerization

To verify that step 1) and 2) in the CASSCF pathway are uncorrelated and independent from each other, i.e., there is not a "shortcut" to bypass the TS1 barrier, we performed additional constrained geometry optimizations with restraining both r_{CN} and θ_{NNCC} in the range of 1.30 to 1.42 Å and 160 to 175 degrees, respectively. A contour plot of the local 2-dimensional potential energy surface is shown in Figure S6(a), where the TS along C=N bond elongation at θ_{NNCC} = 180 degrees is the lowest barrier. A 1-dimensional fit to the potential energies at θ_{NNCC} = 180 degrees using cubic spline interpolation method is shown in Figure S6(b), where the approximation of TS is ~1.6 kcal/mol above the *E,E*-2PyDIG isomer. Since the ensuing transition states are submerged, they are not expected to be kinetically important according to transition state theory. Similarly, additional sampling by restraining both r_{CN} and θ_{NNCC} in the range of 1.30 to 1.42 Å and 0 to 15 degrees showed no correlation between steps 2) and 3).

Reconstruction of Time-Resolved Fluorescence Spectra

To qualitatively visualize how time-resolved fluorescence spectra evolve during the photoisomerization, we performed spectral reconstruction using the TCSPC data shown in Figure 4 and Figure 7, respectively. In view of the strong overlap between the emission spectra of the *E,E* and *Z,Z* isomers shown in Figure 1b and their unknown relative contributions to the TCSPC data measured upon excitation at either of the excitation pulses centered at 336 and 356 nm, we assume that the *Z,Z* isomer is the dominant electronic excited-state species and thus took the emission spectrum acquired upon 60 min illumination (see Figure 1b) as the steady-state fluorescence spectrum for this spectral reconstruction. The resulting reconstructed time-resolved spectra are shown in Figure S4a and S4b, respectively. A remarkable difference between these spectra is the presence of a clear rise in the fluorescence emission at the short wavelength region in the spectra in Figure S4a. It should be emphasized that use of a different steady-state spectrum for this reconstruction will unavoidably alter the shape of the time-resolved fluorescence spectra, but this rise feature will remain in the resulting time-resolved fluorescence spectra.

2. Supplementary Figures

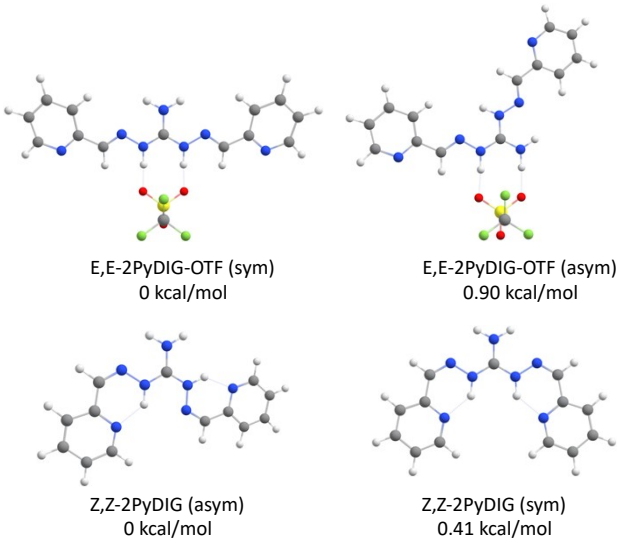

Figure S1. Relative free energies of triflate (OTF) complexes with 2PyDIG in the *E,E* form and free ligands in the *Z,Z* form in DMSO solvent. The structures are optimized using the M06-2X/def2TZVPP method followed by single-point energies computed at the DLPNO-CCSD(T)/cc-pVTZ level.

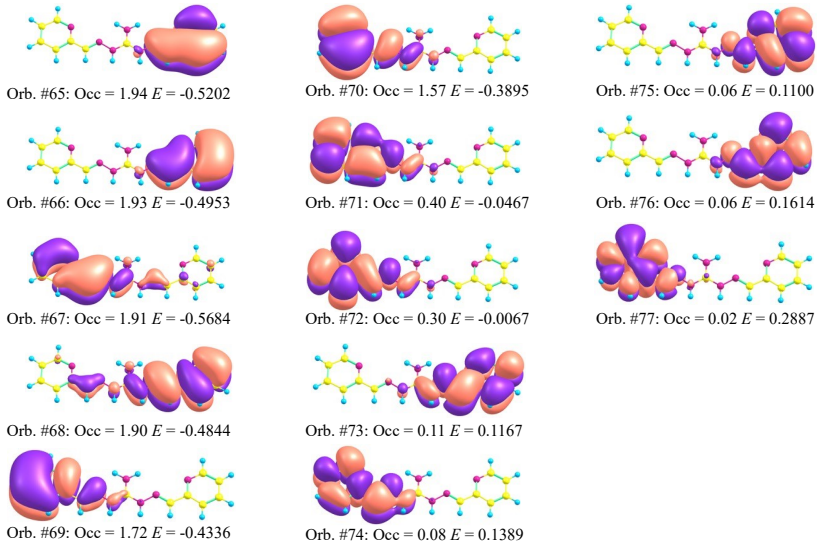

Figure S2. The CASSCF active orbital rendered at 0.01 isosurface, electron occupations, and orbital energies of the optimized *E,E* isomer at SA2-CAS(13,12)SCF/6-31G** level of theory.

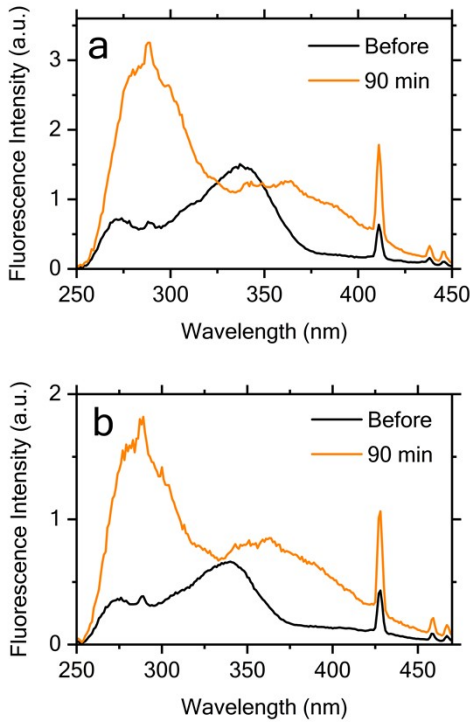

Figure S3. Steady-state fluorescence excitation spectra before and after light illumination to induce the *E,E* → *Z,Z* photoisomerization using a xenon lamp for 90 minutes. The emission wavelength was 468 nm (a) and 491 nm (b), respectively, and the spectra were normalized by the corresponding maximum sample absorbance. These spectra exhibit a qualitatively similar but more pronounced difference, where a dominant contribution from the *Z,Z* isomer is observed from ~270 to ~ 320 nm and from ~355 to the longest excitation wavelength used for the measurement, whereas both *E,E* and *Z,Z* isomers contribute similarly between these two spectral regions. The sharp peaks at 428 nm arise from DMSO Raman scattering.[1]

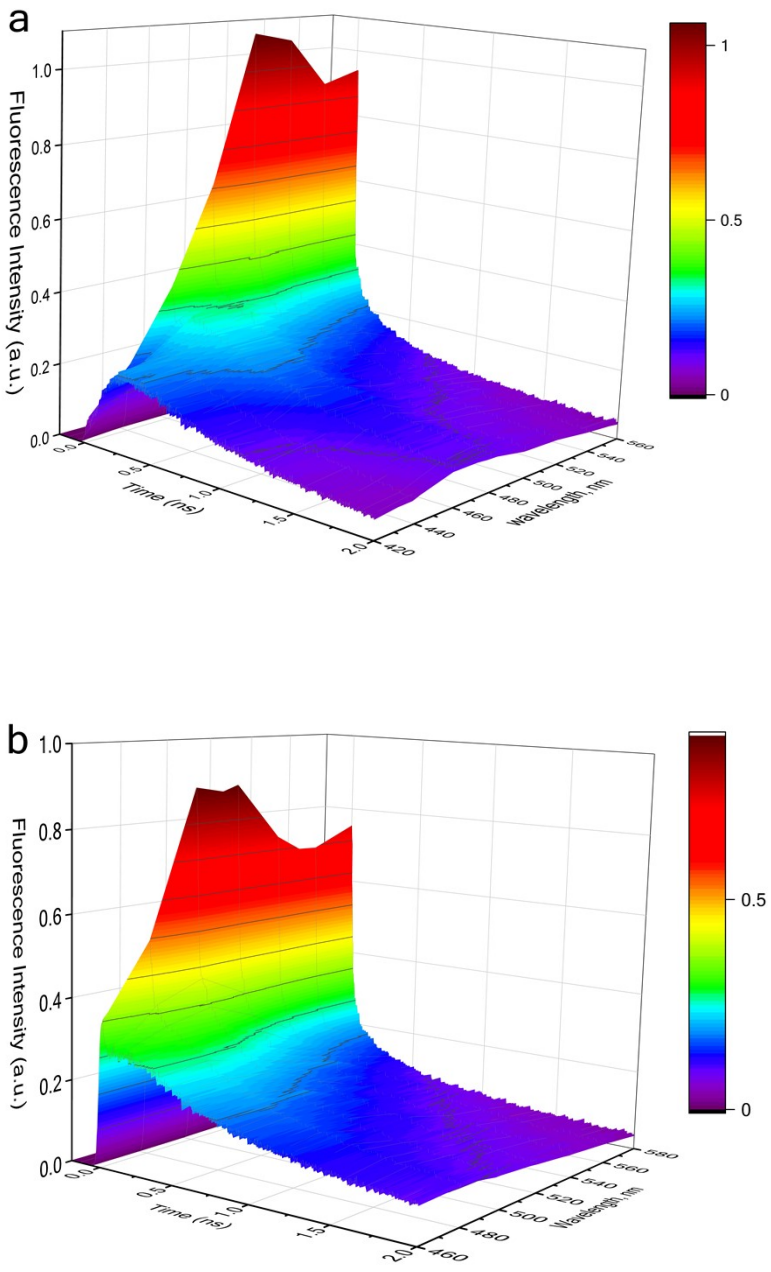

Figure S4. Reconstructed time-resolved fluorescence spectra using the TCSPC data measured upon excitation at 356 nm (a) and 336 nm (b), respectively.

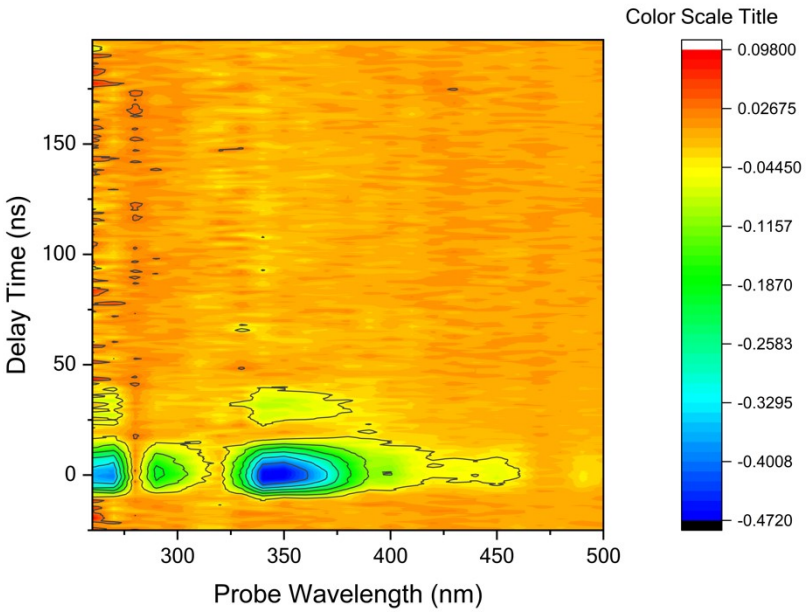

Figure S5. Contour plot of transient absorption signal versus probe wavelength and delay time obtained upon optical excitation with a nanosecond laser at 355 nm.

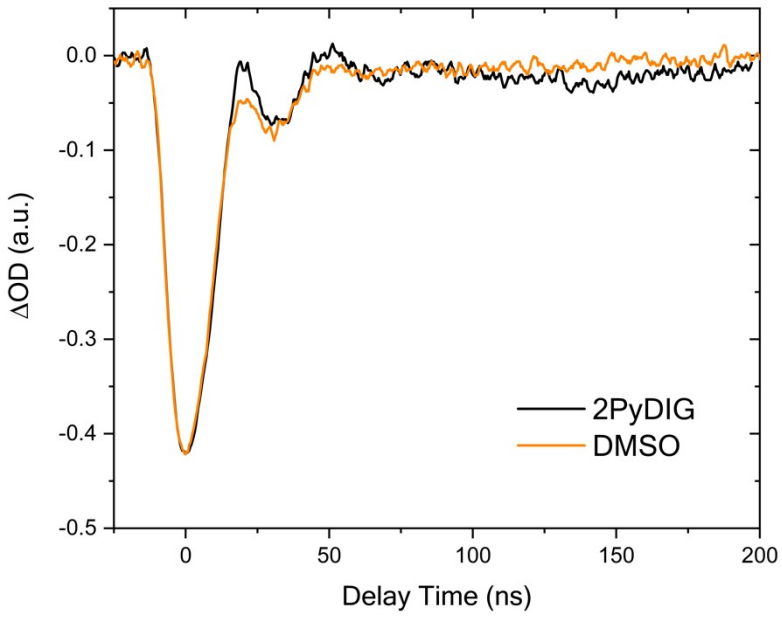

Figure S6. Nanosecond transient absorption kinetics acquired for 2PyDIG/DMSO solution and pure DMSO solvent at 360 nm. To ease comparison, the data are scaled to an equal amplitude at time-zero.

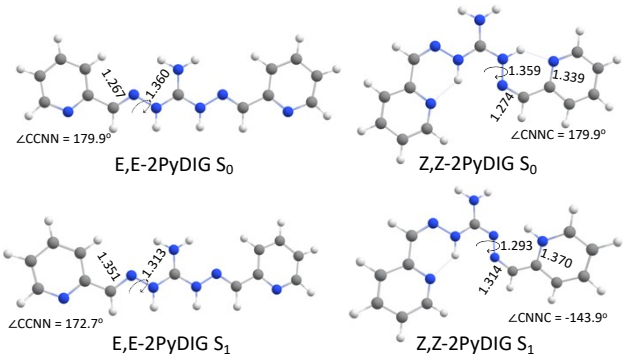

Figure S7. Optimized structures of the most stable conformers of the *E,E* and *Z,Z* forms and the selected geometric parameters in the ground (S_o) and the first excited (S_1) states obtained using TD-DFT theory at the CAM-B3LYP/def2TZVP level.

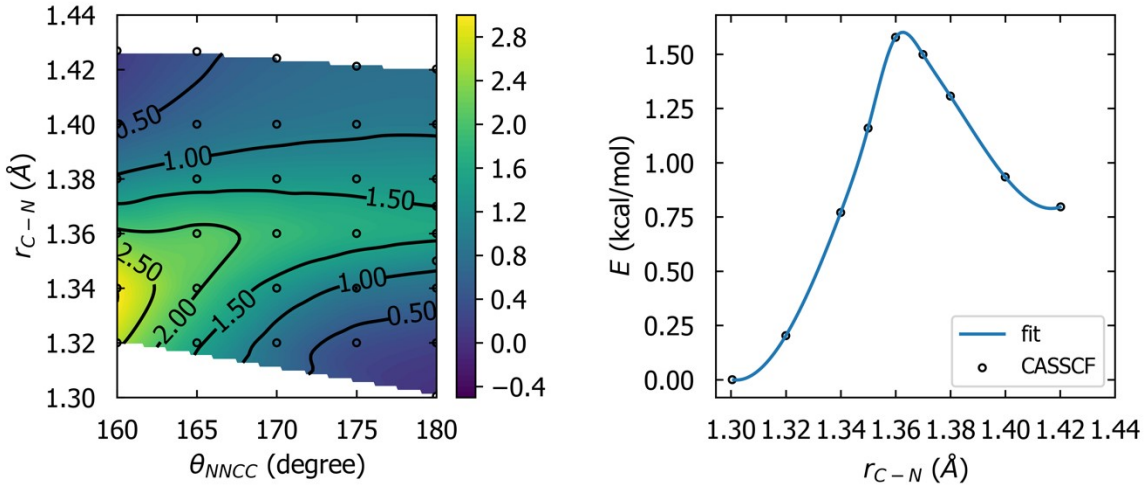

Figure S8. a) 2-Dimensional potential energy surface (PES) of the *E,E*-2PyDIG isomer in S_1 electronic excited state as a function of C–N distance and N-N-C-C dihedral angle. Each hollow dot represents a result of a 2-dimensional constrained geometry optimization at CASSCF/6-31G** level of theory, in

which the orthogonal degrees of freedom are relaxed. Both the contour map as well as the heat map (energies are in kcal/mol, are calculated from a 2-dimensional interpolation of the CASSCF results. b) The potential energies at θ_{NNCC} = 180 degrees as a function of C=N distance. In both plots, the energy of the optimized *E,E*-2PyDIG isomer is 0.

3. Supplementary Reference

1. W. N. Martens, R. L. Frost, J. Kristof and J. Theo Kloprogge, Raman spectroscopy of dimethyl sulphoxide and deuterated dimethyl sulphoxide at 298 and 77 K, *J. Raman Spectroscopy*, 2002, **33**, 84-91.